Modeling of Neon Tube Powered by High Frequency Converters

Shan Lu, Zhongyuan Cheng, Bin Wu
Department of Electrical and Computer Engineering,
Ryerson University
350 Victoria Street, Toronto, Ontario, Canada M5B 2K3
glu@ee.ryerson.ca gcheng@ee.ryserson.c bwu@ee.ryserson.ca

Reza Sotudeh
Department of Electrical and Electronics Engineering,
University of Hertfordshire
College Lane, Hatfield, Herts, UK AL10 9AB
R.Sotudeh@hets.ac.uk

Abstract – **This paper presents a dynamic model for neon tubes. The model is derived from conventional Cassie's and Mayr's equations which are often used to model low-voltage and high-current arc discharges, such as electrical arcs in switching interrupters and HID lamps. In this paper, the effects of various types of energy dissipation mechanisms on conductance of the plasma channel are considered for high-voltage and low-current neon tubes. In particular, the Cassie's and Mayr's equations are modified such that the loss on the heat conduction of the neon tube can be accurate modeled. Some basic rules for the selection of parameters in the model are proposed. Simulation is performed using Pspice simulator. A high frequency switch mode supply is built to power the neon tube under test. Experimental results reveal that the developed neon tube dynamic model is applicable for both low and high frequency operations.**

I. INTRODUCTION

Dynamic models for neon tubes are essential for optimum design of high efficiency transformers and driving circuits. However in a survey of existing models for gas discharge lamps, it has been found that little has been done for neon tubes. Based on the knowledge that both neon tubes and fluorescent lamps are of glow-discharge type[1], it is hopeful to develop a model for neon tubes based on those for fluorescent lamps.

Most mathematic models consider the fluorescent lamp as a lumped nonlinear device. These models do not take into account the lamp physical process, which is critical and essential to the lamp performance. The existing models may be sorted into the following four categories:

(1) Polynomial models including constant resistor, parabolic and cubic models. In the constant resistor models, the lamp is simply treated as a fixed resistor whose value can be calculated from its operating point on the static V-I curve. Thomas and John Richard proposed a parabolic model[2] in which the lamp voltage is a function of the 2nd power of lamp current. The parabolic models can be used to obtain a set of lamp parameters for specific current waveforms. U. Mader and P. Horn[3] proposed the well-known cubic model which contains coefficients as functions of lamp power. M. Sun. modified the cubic model for accuracy and avoiding divergence[4]. Chin S. Moo et al. used separate polynomial equations for both current and voltage for the convenience of simulation[5]. Models with polynomials higher than the 3rd order may also be deduced from experimental data but it is unnecessary in view of both accuracy and validity.

(2) Sectional approximation models. E.M Gluskin proposed a piece-wise linear model in which the voltage is a function of current polarity[6]. This model is more suitable for use with high tube current. M. T. Abuelma'atti suggested three different functions for the three regions of the I-V curve[7]. Sectional approximation models are generally for fluorescent lamps operating at low frequencies such as 60HZ.

(3) Variable resistor models. In these models the effective resistor of the lamp is inversely proportional to the rms(root mean square) value of the lamp current (I_{rms})[8]. The model reflects the fact that the current increase will cause an increase in the plasma density thus the lamp conductance. T. F. Wu et al.[9] and S. Ben-Yaakov[10] developed and improved a Pspice compatible model based on this idea, which included a continuous integrating algorithm for I_{rms}. These models are generally for fluorescent lamps operating at high-frequencies.

(4) Differential conductance/resistor models. To some extent these models take into account the plasma processes inside the lamp and can be used for dynamic simulation. M. Tola[11,12] established a differential model based on V. J. Francis' work[13]. In this model, the differential conductance is determined by the difference between two polynomials, one is a function of the 2nd order bivar polynomials of i and v, and the other is the 3rd order polynomials of conductance. K. J. Tsing[14] and T. Lin [15] used traditional Cassie's and Mayr's equations which are often used to calculate electrical arc discharges. While K. J. Tsing used Mayr's equation for lower current discharges and Cassie's equation for higher current discharges respectively[14], T. Lin used the sum of the two[15]. All these models were developed used for dynamic simulation of fluorescent lamps. The neon tube model presented in this paper falls into this category as well.

It should be noted that the plasma parameters and inner processes in neon tubes and fluorescent lamps differ from each other[1], leading to different I-V characteristics, despite the fact that both are low pressure glow-discharge lamps. This means that the models for fluorescent lamps cannot be directly utilized for neon tubes.

Before modeling the neon tube, we tried to use the model presented in ref.[15]. But it seemed that this model doesn't give reasonable results. One possible reason is that the conductance of the neon tube can not be obtained by simply adding Cassie's and Mayr's equations together without considering the energy balance inside the tube, which is the case of ref.[15].In order to build an accurate model for neon tubes, a dynamic model is proposed in this paper, which is

0-7803-7474-6/02/$17.00 ©2002 IEEE

also based on Cassie's and Mayr's equations. Section II introduces the model with discussion on the energy balance of the neon tube. In Section III the parameters in the model are deduced based on the proposed rules. Pspice simulation results and experimental waveforms are given in Section IV. Section V gives the conclusions.

II. MODELING

In Cassie's equation, the energy dissipates mainly on convection including the deformation of the discharge channel, which is proportional to the cross-sectional area of the channel. The discharge channel is regarded as a columnar plasma body with a uniform temperature distribution along the radius and a constant electrical field along the axis. Cassie's equation can be expressed as:

$$g = \frac{ui}{U_0^2} - \theta_1 \frac{\mathrm{d}g}{\mathrm{d}t} \tag{1}$$

where g is the dynamic conductance, u the instantaneous tube voltage, i instantaneous tube current, U_0 a constant with a voltage dimension, and θ_1 a time constant which equals to the ratio of energy per volume to the power dissipation per volume.

In Mayr's model, the energy dissipates on heat conduction including radial diffusion at a constant rate. The discharge channel is a columnar plasma body with constant radius. Mayr's equation can be written as:

$$g = \frac{i^2}{P_0} - \theta_2 \frac{\mathrm{d}g}{\mathrm{d}t} \tag{2}$$

where P_0 is the constant power of heat conduction, θ_2 the time constant after which the plasma conductance changes to 2.73 times of its original value.

However, both Cassie's and Mayr's model considered only one type of energy thermal dissipation mechanism, which was far from the actual picture. Cassie and Mason put a more complicated model with consideration of both thermal conduction and convection and obtain the following equation:

$$\frac{\mathrm{d}g}{\mathrm{d}t} = g\frac{K}{d^2}(p - \beta Q - p_0) \tag{3}$$

where K and β are constants, d the variable diameter of plasma channel, Q the heat accumulated in the plasma region, βQ the convection term and p_0 the conduction term. Eq.3 is difficult to be solved because d and Q are also variables. However it gives some hints to building the model, i.e. the neon tube can be modeled based on analyzing the energy balances.

In fact both Cassie's and Mayr's equations can be derived from Eq.3 with certain assumptions. For neon tubes, there should be three main mechanisms of energy dissipation, i.e. conduction, convection and radiation. It is assumed that the three mechanisms correspond to different plasma conductivity. As mentioned above, conductance corresponding to conduction and convection can be described by Eqs. (1) and (2) respectively. Actually, the power of thermal conduction between plasma border (with a radius of $d/2$ and temperature T) and a given columnar surface (with a radius of $d_0/2$ and room temperature of T_0) is[16]:

$$P_{cond} = \frac{2\pi\lambda(T - T_0)}{\ln(d_0/d)}$$

where λ is a constant. For a given temperature difference, P_{cond} tends to be a constant, which coincides to the assumption of Mayr's model, i.e.

$$P_{cond} = P_0 \tag{4}$$

For a given temperature difference, the convection term is proportional to the cross-sectional area[16], i.e.

$$P_{conv} = 0.322 d^2 v \ln\frac{T}{T_0} \propto K_{conv} A \tag{5}$$

where K_{conv} is a constant and A the cross-sectional area of the channel. It coincides with Cassie's model.
As to the radiation term, we have[16]

$$P_r = 71.6(\frac{d}{2})^2 l\varepsilon\,[(\frac{T}{1000})^4 - (\frac{T_0}{1000})^4] \propto K_r A \tag{6}$$

where l is the length of the plasma channel, ε and K_r are constants. Radiation power meets the assumption of Cassie's model.

As Eqs. (4)~(6) coincide with Mayr's and Cassie's assumptions, we can use Eq.(1) and (2) to model the neon tube under the following assumptions:

(1) The energy input to the plasma is balanced by thermal conduction, which leads to a plasma conductance described by Mayr's equation, and convection and radiation, which lead to the conductance described by Cassie's equation.

(2) A fraction (α) of the total current (i) passing through the tube corresponds to the energy loss of heat conductive, i.e. i_{cond} in Eq.(7). The remaining ($1-\alpha$) of the current compensates the energy loss of convection and radiation, i.e. i_{conv+r} in Eq.(7). We have

$$\begin{cases} i_{cond} = \alpha i \\ i_{conv+r} = (1-\alpha) i \end{cases} \tag{7}$$

(3) The overall conductance of the tube is the sum of the conductance corresponding to different energy dissipating mechanisms.

From Eqs. (1), (2) and (7), we have

$$\begin{cases} g_1 = \dfrac{\alpha\, iu}{V_0^2} - \theta_1 \dfrac{\mathrm{d}g_1}{\mathrm{d}t} + g_0 \\ g_2 = \dfrac{(1-\alpha)^2 i^2}{p_0} - \theta_2 \dfrac{\mathrm{d}g_2}{\mathrm{d}t} + g_0 \end{cases} \tag{8}$$

where g_0 is a minute conductance which is necessary to initiate Pspice calculation.
To simulate the tube in Pspice, we also have:

$$\begin{cases} g = g_1 + g_2 \\ u = i/g \end{cases} \tag{9}$$

Before using Eqs.(8) and (9) to simulate neon tubes, the parameters in Eq.(8) must be carefully selected.

Fig.1 shows the block diagram of the Pspice neon tube model.

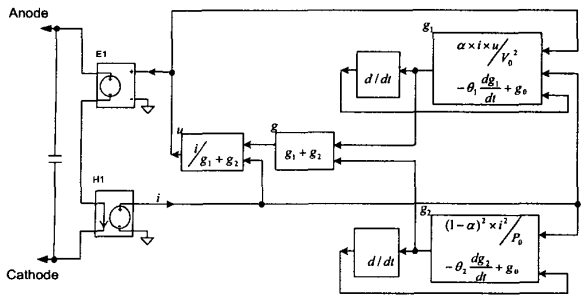

Fig.1 Block diagram of neon tube modeling

III. PARAMETERS SELECTION

To use the model, the parameters in the model must be first determined for neon tubes in certain circuit sets. The parameters can be determined by fitting the simulating results to experimental data of low-frequency voltage waveforms or low-frequency envelope of modulated voltage waveforms. Fig.2 schematically shows a half cycle of the low-frequency voltage waveform of the neon tube. The waveform may be characterized by the following three points: striking peak (v_1, t_1), sag point (v_2, t_2) and extinguishing peak (v_3, t_3).

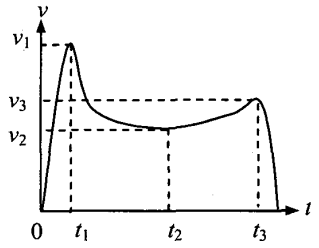

Fig.2 Characterizing of voltage wave form of a neon tube

All the parameters in Eq.8, α, V_0, P_0, θ_1 and θ_2, can be determined by the following steps:

(1) Choose α according to the striking/sag-voltage ratio V_1/V_2 as shown in Fig.3, or according to the empirical formula of $V_1/V_2=0.36+43.8e^{-4\alpha}$. Fig.4 shows tube voltage changing with α.

(2) Choose θ_1 according the striking/extinguishing voltage ratio V_1/V_3 as is shown in Fig.5, or according to the empirical relation of $V_1/V_3=0.9+126.3\theta_1^{1/2}$. Fig.6 shows the voltage waveform changing with θ_1.

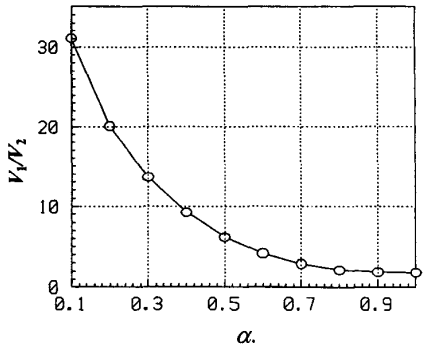

Fig.3 Relationship between Striking/sag voltage ratio and coefficient α

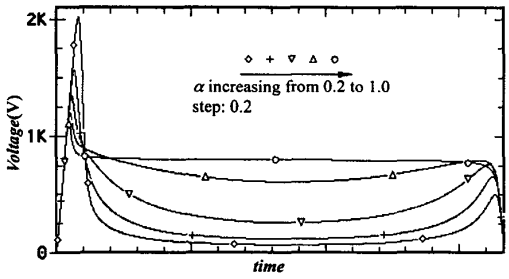

Fig.4 Effects of α on tube voltage waveform

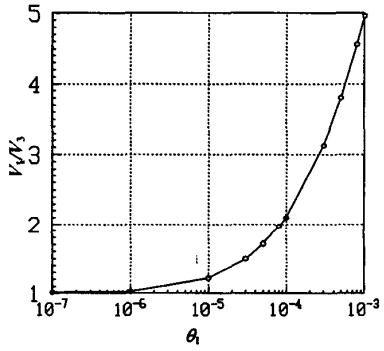

Fig.5 Striking/extinguishing voltage ratio Versus θ_1

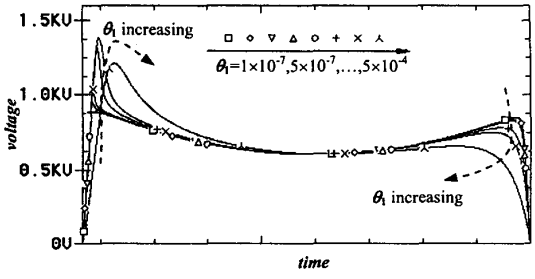

Fig.6 Effects of θ_1 on tube voltage waveform

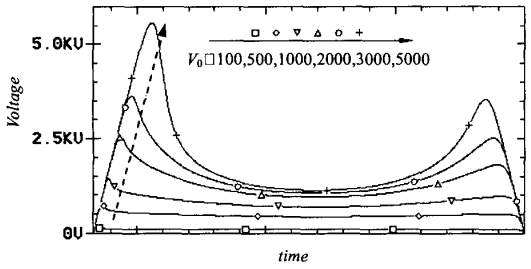

Fig.7 Voltage waveforms changing with V_0

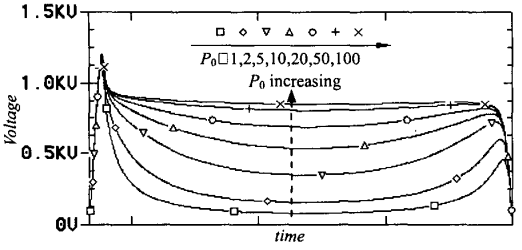

Fig.8 Voltage waveforms changing with P_0

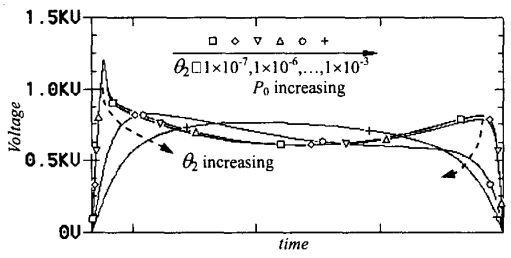

Fig.9 Voltage waveforms changing with θ_2

(3) Choose V_0 so that V_1 coincides with the experimental data. Generally V_1 increases with increasing V_0. Fig.7 shows the change of voltage waveforms with increasing V_0.

(4) Choose P_0 so that V_2 coincides with the experimental data. V_2 increases with increasing P_0. Fig.8 shows the change of voltage waveforms for different P_0.

(5) choose θ_2 so that V_3 coincides with the experimental data. The value of θ_2 should be less that 1×10^{-3}, and its influence on V_3 will almost be diminished for a value less than 1×10^{-5}. V_3 decreases with increasing θ_2. Fig.9 shows voltage waveforms influenced by θ_2.

(6) repeat (3)~(5) to adjust the parameters for precision.

In most cases, the initial value may be chosen as P_0=10, α=0.7, $\theta_1=\theta_2=1\times10^{-5}$, $G_0<1\times10^{-7}$ while the choice of V_0 may greatly dependent on whether primary or secondary equivalent circuit is used for simulation. In the case of secondary-side simulation, the initial value of V_0 can be $(0.2\sim1.0)V_1$. While in the case of primary-side simulation, V_0 can be the 0.2~1.0 times striking voltage divided by transformer ratio.

IV. SIMULATION AND EXPERIMENTS

Fig.10 shows a Pspice model for a neon tube powered by a high frequency converter through a step-up transformer. The diode rectifier converts the utility power superbly of 60Hz to a dc voltage. A half bridge MOSFET inverter is used to convert the dc voltage to a high frequency ac voltage. The MOSFETs are simulated by a pair of voltage controlled switches operating at a switching frequency of 21KHz with a 50% duty cycle. The use of a half-bridge instead of a full bridge is mainly for the manufacturing cost reduction.

The step-up transformer has a turns ration of 64 with a nominal secondary voltage of 9000V. The transformer is designed with a high leakage inductance which can effectively limit the current in the neon tube. The transformer TX1 shown in Fig.5 is an ideal transformer, whose magnetizing inductance, leakage inductance, and winding resistances are represented by L2, L3, L4, R3 and R5, respectively. The use of high frequency transformed further reduces the physical size and weight of the neon tube power supply.

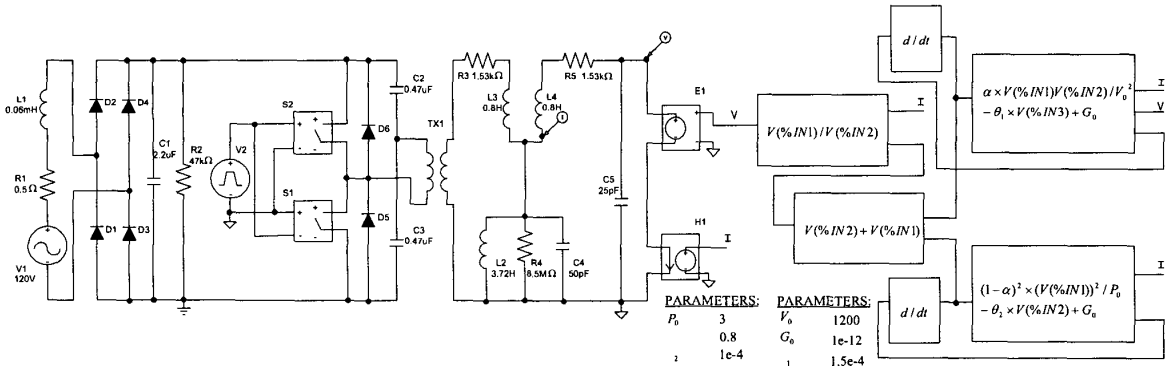

Fig.10 Schematic drawing of neon tube coupled with a transformer for Pspice simulation

The neon tube is modeled by ABM (Analog Behavior Modeling) components in Pspice. The ABM component in Pspice allows a mathematical relationship to be used to model a circuit segment so that the segment needs not be designed component by component.

It should be point out that the DC filter capacitor C1 should be made as small as possible for reduction in manufacturing cost. In the simulation, we choose C1 as 2.2uF. Also the capacitors C2 and C3 in the half-bridge converter are in small value as 0.47uF. These yield the 60Hz contour in the output voltage.

Following the steps in Section III, a set of experimental parameters for the tube model is determined by fitting the simulation results to the 60Hz envelope.

An experimental system was set up to obtain real time voltage and current waveforms. The tube in the experiment is a five-foot red neon with a diameter of 15mm. A high voltage transformer is powered by an AC-DC-AC converter with a frequency of 21 kHz.

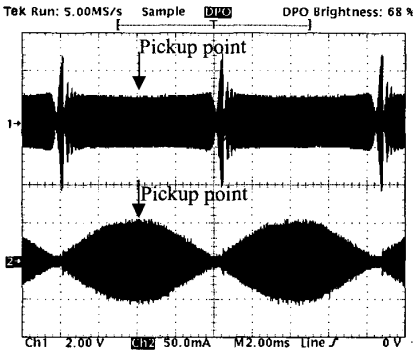

(a) Experimental waveforms
Upper trace: voltage. Lower trace: current

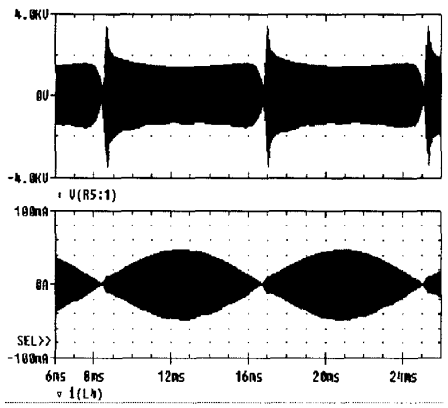

(b) Simulation waveforms

Fig.11 Experimental and simulating results of neon tube
Upper trace: voltage. Lower trace: current

The voltage waveform of the tube is shown in Fig.11 (a), which is composed of high frequency components with a 60Hz contour. Note that the voltage waveform in Fig.11 (a) was measured by a high-frequency voltage probe with an attenuation coefficient of 1000:1 thus the effective scale voltage is 2kV/div. Fig.11 (b) shows the simulating results. Both the current and the voltage fits well with Fig.11 (a) except the several ignition peaks at the beginning of each cycle.

It should be pointed out that from Fig.11 (a) the discharge is not stable in the ignition stage thus there are several striking voltage peaks at the beginning of each cycle. The instability may be due to the phenomenon of the breakdown of gas discharge, which is out of the scope of this paper. However, the first striking peak, which is important to transformer and wiring design, can be simulated with acceptable precision.

Cassie's and Mayr's equations have been most often used to simulate arc discharges in interrupters which are featured by low voltage and very large current. This is why the amplitude of tube voltage will always be smaller than the actual value when only one of the equations is used. T. Lin et al[15] applied some assumptions for as-called 'anode voltage' (actually it should be cathode voltage) which leads to a conductance of:

$$G_a = \frac{G_p}{\alpha|i^2|+\beta} + G_{opn}.$$

However, simulation turns out that above expression is not applicable for neon tubes. In the present model it is unnecessary to consider cathode voltage separately. In view of energy balance, the energy produced by the cathode potential drop is the same as that produced by positive column. Eqs. (3) and (8) include all kind of energy input to the neon tube.

The model is suitable for both high and low frequencies. To check the high frequency performance, a cycle of high frequency component was picked from Fig.11, which are chosen at the current peaks (*i.e.* the corresponding pickup points in Fig.11) when the discharge is the most stable. Fig.12 is the V-I characteristics of the pickup cycle. Fig.12(a) is the experimental results of the V-I characteristic of a high frequency operation cycle. It shows the hysisteresis of the V-I characteristic, which is always be assumed neglectable in most of the literatures. Fig.12(b) shows the simulation results of V-I characteristic of neon tube high frequency operation. The hysteresis is properly simulated. The simulated V-I characteristics are somewhat more linear than practical situation. This is mainly caused by the nonlinear property of the neon tube, which is not fully considered in the model.

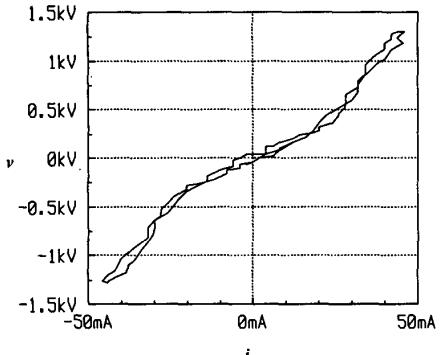

(a) Experimental I-V curve

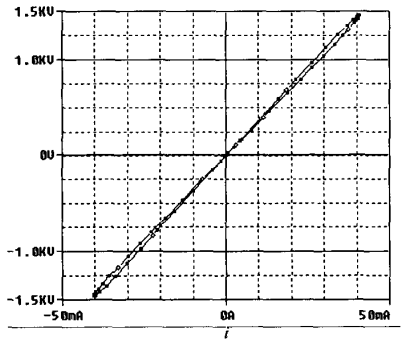

(b) Simulation I-V curve

Fig.12 Comparison of high-frequency characteristics of the tube

V. CONCLUSIONS

A Pspice neon tube model is proposed in this paper by using Cassie's and Mayr's equations, which are traditionally for the modeling of electrical arc discharge process. In order to develop a practical model for the analysis of new tubes, which belong to glow discharge process, these two equations are modified such that they can take into account various energy dissipation mechanisms such as convection, radiation and conduction energy losses. A systematic method is developed to determine the coefficients of the modified equations. The proposed model is particularly suitable for use in simulation where a high frequency switch mode converter is used. Experimental results demonstrate that the model is able to predict the dynamic characteristic of neon tube for both high and low frequency operation.

VI. REFERENCES

[1] James T. Dakin, "Nonequilibrium lighting plasmas", IEEE Trans on Plasma Sci., Vol.19, No.6, 1991, pp.991-1002

[2] Thomas J. Ribarich and John. J. Ribarich, "A new high-frequency fluorescent lamp model", IEEE IAS 1998.

[3] U. Madar and P. Horn, "A dynamic model for the electrical characteristics of fluorescent lamps", IEEE IAS 1992, Vol.2, pp1928-1934.

[4] Mark Sun and Bryce L. Hesterman, "Pspice high-Frequency dynamic fluorescent lamp model", IEEE Trans. Power Electronics, Vol.13, No.2, 1998

[5] Chin S. Moo, Ying C. Chuang, Yung H. Huang and Horn N. Chen, "Modeling of fluorescent lamps for dimmable electronic ballast", IEEE IAS, Vol/4, 1996, pp.2239-2236

[6] Emanuel Gluskin, "The non-linear theory of fluorescent lamp circuits", Int. J. Electronics, 1987, Vol/63, No.5, pp.687-705

[7] Muhammad T. Abuelma'atti, "Modeling the current-voltage characteristics of a fluorescent lamp to computer-aided design", Int. J. Electronics, 1989, Vol.66, No.5, pp.835-pp.839

[8] M. Gulko and S. Ben-Yaakov, "Current-sourcing parallel resonance inverter(CS-PPRI)": Theory and application as a fluorescent lamp driver", in Proc. IEEE APEC'93, pp.411-417

[9] T.-F. Wu, J.-C. Hung and T.-H. Yu, "A Pspice model for low-pressure gaseous discharge lamps operating at high frequency", IEEE Trans. Ind. Electron., Vol.44, pp.428-431, 1997

[10] S. Ben-Yaakov, "Modeling the high-frequency behavior of a fluorescent lamp: a comment on 'A Pspice model for low-pressure gaseous discharge lamps operating at high frequency'", IEEE Trans. Ind. Electron., Vol.45, No.6, 1998

[11] Muhammad Tola, Kimihiko Nkamura and Hiroshi Bo, "An investigation of the model constants for the fluorescent lamps with resistance ballast circuit", J. Light & Vis. Env., Vol.9, No.1, 1985

[12] Muhammad Tola, Kimihiko Nkamura and Hiroshi Bo, "Model equations of fluorescent lamps on the high frequency operation", J. Light & Vis. Env., Vol.10, No.1, 1986

[13] V. J. Francis, "Fundamental of discharge tube circuit", John Wiley, 1948

[14] K. J. Tseng, "Dynamic model of fluorescent lamp implemented in Pspice", Power Conversion Conference - Nagaoka 1997., Proceedings of the , Volume: 2 , 1997, pp.859-864

[15] T. Lin, K. J. Tseng and D. M. Vilathgamuwa, "A Pspice model for electrical characteristic of fluorescent lamps", IEEE PESC'98, 1998, pp.17-22

[16] Zhang Guansheng, ed "Fundamental Theory of Electrical Apparatus", China Machine Press, Beijing, 1983